ADVANCED FUNCTIONAL MATERIALS
www.afm-journal.de

Direct Measurement of Raman Scattering Tensor of Orientation-Fixed Single Iodine Molecules

*Dingdi Wang and Zikang Tang**

Raman spectroscopy is the most widely used noninvasive analytical technique. Apart from the fingerprint Raman frequency for identifying vibrational mode of certain functional groups, the Raman scattering tensor can also be used to determine the corresponding vibrational symmetry as well as the orientation of this functional group with respect to the rest of the molecule. For gaseous single molecules, only limited structural information can be obtained from Raman spectroscopy owing to their freely rotating and randomly oriented nature. Here, a method, for the first time, is developed to directly determine the Raman scattering tensor on orientation-fixed single iodine molecules, which are confined inside the nano-sized channels of zeolite $AlPO_4$–11 (AEL) single crystal. The experimental results are in good agreement with theoretical predictions based on a density functional theory. The optical transparency and appreciable size of the crystal facilitate the Raman exploration and the 3D manipulation. It is also demonstrated that iodine molecules' orientations are randomly distributed inside the nano-channels of $AlPO_4$–5 (AFI) crystal, which indicates that by carefully choosing the relevant zeolite crystal, the big family of zeolites can be utilized as directing template database for orienting a large number of guest molecules to estimate their structures by polarized Raman spectroscopy.

1. Introduction

The world around us is built up by chemical bonds, whose equilibrium length in a crystal can be estimated by X-ray or neutron diffractions and vibrational behavior can be well-described by Raman spectroscopy. The vibrational symmetry can be determined by the Raman scattering tensor α', which can be expressed as

$$\alpha' = \begin{bmatrix} \alpha'_{xx} & \alpha'_{xy} & \alpha'_{xz} \\ \alpha'_{yx} & \alpha'_{yy} & \alpha'_{yz} \\ \alpha'_{zx} & \alpha'_{zy} & \alpha'_{zz} \end{bmatrix} \quad (1)$$

Each component $\alpha'_{\rho\sigma}$ (ρ, σ = x, y or z) can be measured separately for experimental geometries in which the scattering and excitation lights are polarized along the ρ-axis and σ-axis, respectively. According to the group theory, the form of the Raman scattering tensor of each vibrational mode can well describe the corresponding vibrational symmetry species and can be used to verify the crystal axes,[1,2] such as for ZnO crystal,[3] BeO crystal[4] and TiO_2 crystal.[5] For low-dimensional macromolecule such as carbon nanotubes, apart from estimating its radius from the vibrational frequency of radial breathing mode, polarized Raman spectroscopy can also be used to confirm the nanotube's orientation,[6–8] or even to determine the curvature effect induced force constant difference between vibrations along the nanotube axis and circumferential direction.[9]

For single molecules, in theory polarized Raman spectroscopy can provide richly useful information on the molecular shape such as determining the orientation of each functional group with respect to the rest of the molecule,[10] but only limited structural information can be obtained because gaseous single molecules are freely rotating and randomly oriented. The Raman scattering tensor of single molecules can only be derived by complicated conversion from polarized Raman scattering experiment on oriented single crystals of known molecular structure.[10] Thus, the Raman scattering tensor only plays a secondary role and serves as a supplementary method to corroborate the molecular structure.[11] Instead of common X-ray and neutron diffractions, the equilibrium structure of one single molecule has to be resolved at temperature near absolute zero by the special atomic force microscopy.[12] The Raman spectrum of one single molecule still cannot be observed directly due to the extremely low signal strength. It has been demonstrated that single-molecule sensitivity can be achieved with the help of surface-enhanced Raman scattering technique,[13,14] and Raman polarization behavior in certain direction has been observed,[13,15] but owing to the fact that the molecule is attached to silver nanoparticle or

Dr. D. Wang
State Key Laboratory on Integrated Optoelectronics
College of Electronic Science and Engineering
Jilin University
Changchun 130012, China
Dr. D. Wang
Department of Physics
The Hong Kong University of Science and Technology
Clear Water Bay
Kowloon, Hong Kong
Prof. Z. K. Tang
The Institute of Applied Physics and Materials Engineering
University of Macau
Avenida da Universidade
Taipa, Macau
E-mail: zktang@umac.mo

DOI: 10.1002/adfm.201500763

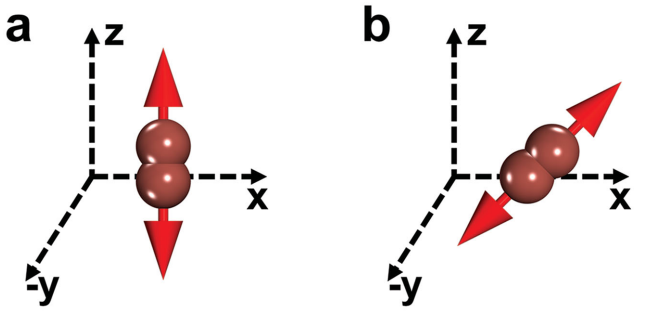

$$\alpha'_z = \begin{bmatrix} -0.088 & 0 & 0 \\ 0 & -0.088 & 0 \\ 0 & 0 & -0.451 \end{bmatrix} \qquad \alpha'_{z\text{-}45^\circ} = \begin{bmatrix} -0.269 & 0 & -0.181 \\ 0 & -0.088 & 0 \\ -0.181 & 0 & -0.269 \end{bmatrix}$$

Figure 1. The vibrational modes and calculated Raman scattering tensors of iodine molecules oriented a) along *z*-axis and b) 45° with respect to the *z*-axis and *x*-axis.

deposited on metal substrate the complete determination of the molecule's Raman scattering tensor remains elusive.

If we can create a kind of "oriented gas," which can be easily manipulated three-dimensionally and consists of billions of independent single molecules with the same orientation, the problem will be solved since its Raman tensor will be the same as that of one molecule and the signal strength is detectable. In this article, we focused on using the nano-channels of aluminophosphate ($AlPO_4$-*n*) zeolite single crystals to control the orientations of iodine diatomic molecules occluded.

The iodine molecule, which is a diatomic molecule, belongs to the $D_{\infty h}$ point group and has only one vibrational mode (A_{1g}). As exemplified in **Figure 1**a, if the iodine molecule is oriented along the z-axis, only $\alpha'_{xx} = \alpha'_{yy} \neq 0$ and $\alpha'_{zz} \neq 0$ will hold, according to group theory which dictates whether a component is zero or nonzero.[1,2] The recent developing first-principles density functional theory (DFT) calculation can be used to further calculate the values of these components,[16] which serves as a complement to the rigorous group theory and can be compared with the experimental results directly. The DFT calculated Raman scattering tensor of the iodine molecule mentioned above can be expressed as

$$\alpha'_z = \begin{bmatrix} \alpha'_\perp & 0 & 0 \\ 0 & \alpha'_\perp & 0 \\ 0 & 0 & \alpha'_\parallel \end{bmatrix} = \begin{bmatrix} -0.088 & 0 & 0 \\ 0 & -0.088 & 0 \\ 0 & 0 & -0.451 \end{bmatrix} \quad (2)$$

where $\alpha'_{xx} = \alpha'_{yy} = \alpha'_\perp = -0.088$, and $\alpha'_{zz} = \alpha'_\parallel = -0.451$, the unit is Å^2. The detailed discussion of the relationship between the Raman tensors of different vibrational modes and the molecular structures of several small molecules is given in the Supporting Information.

If the iodine molecule is rotated clockwise through angle θ around *y*-axis, according to the tensor transformation rules, the Raman tensor can be calculated as

$$\alpha'_{zx} = \begin{bmatrix} \cos\theta & 0 & -\sin\theta \\ 0 & 1 & 0 \\ \sin\theta & 0 & \cos\theta \end{bmatrix} \begin{bmatrix} \alpha'_\perp & 0 & 0 \\ 0 & \alpha'_\perp & 0 \\ 0 & 0 & \alpha'_\parallel \end{bmatrix} \times \begin{bmatrix} \cos\theta & 0 & \sin\theta \\ 0 & 1 & 0 \\ -\sin\theta & 0 & \cos\theta \end{bmatrix} = \begin{bmatrix} \alpha'_\perp \cos^2\theta + \alpha'_\parallel \sin^2\theta & 0 & (\alpha'_\perp - \alpha'_\parallel)\sin\theta\cos\theta \\ 0 & \alpha'_\perp & 0 \\ (\alpha'_\perp - \alpha'_\parallel)\sin\theta\cos\theta & 0 & \alpha'_\perp \sin^2\theta + \alpha'_\parallel \cos^2\theta \end{bmatrix} \quad (3)$$

As depicted in Figure 1b, the iodine molecule is rotated 45° clockwise in the *xz*-plane, then the related Raman tensor can be calculated from Equation (2) and (3) as

$$\alpha'_{z-45^\circ} = \begin{bmatrix} -0.270 & 0 & -0.182 \\ 0 & -0.088 & 0 \\ -0.182 & 0 & -0.270 \end{bmatrix} \quad (4)$$

which is in good agreement with the one obtained directly from DFT calculations (Figure 1b). Equation (4) shows that besides the diagonal terms, the off-diagonal terms can also become nonzero under rotation. The general Raman experiment on gaseous molecules can only measure the isotropic average of Raman tensor, which is the average value over all directions with the assumption that the molecules are randomly oriented.

In this article, we will show it is feasible to control the orientations of iodine single molecules inside the array of uniform 1D parallel nano-channels of $AlPO_4$-*n* crystals, which are suitable to accommodate small guest molecules.[17–28] The optical analysis of the embedded molecules can be easily conducted on these crystals due to their transparency from ultraviolet to near-infrared.[22–33] According to the dimensions of the nano-channels and the iodine molecules, we have chosen two types of single crystals: $AlPO_4$–5 (AFI) and $AlPO_4$–11 (AEL). We will demonstrate that for iodine-loaded AFI crystal (I_2@AFI), the confined iodine molecules resemble free-rotating gaseous molecules. In contrast, for iodine-loaded AEL crystal (I_2@AEL), iodine molecules can only be oriented along or perpendicularly to the channel axis (oriented gas), then the Raman tensor can be measured directly since iodine molecules' orientations are determinate.

2. Results and Discussion

2.1. The Iodine Molecules' Orientations inside Nano-Channels

The framework structures of the AFI and AEL single crystals have been well-established.[34–36] There are uniform arrays of parallel 1D nano-channels inside the AFI and AEL crystal (**Figure 2**a,d). The main channel of AFI crystal has a circular cross section, which consists of 12 alternating AlO_4 and PO_4 tetrahedrons (Figure 2b). The Connolly surface[37] (or molecular surface) of the nano-channel viewed from the [100] direction is illustrated in translucent blue color in Figure 2c, with the observation direction pointed out in Figure 2a. The diameter of the channel fluctuates between d_l = 8.6 Å and d_s = 7.1 Å due to the inherent arrangement of constituent atoms. Since the length

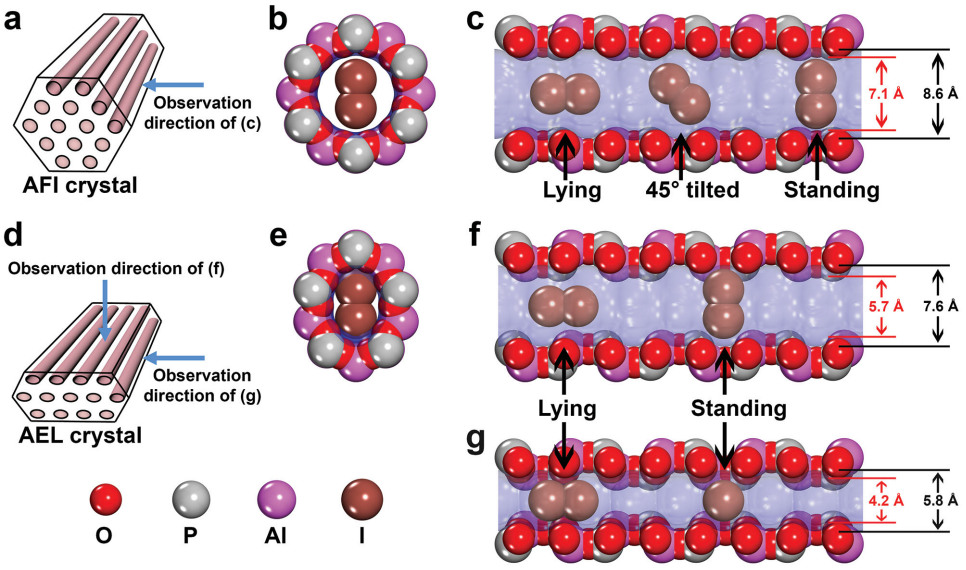

Figure 2. The influence of the diameters of the nano-channels of AFI and AEL crystals on the orientations of iodine molecules embedded. The observation directions of iodine-loaded a) AFI and d) AEL crystals are illustrated. The circular and elliptical cross sections of b) AFI and e) AEL crystal nano-channels are demonstrated. The lateral views of iodine configurations inside the nano-channels of AFI crystal observed from c) [100] direction and AEL crystal observed from f) [010], g) [100] directions are depicted. It reveals that due to the size limitation effect, there is not a preferred orientation or favorite position for iodine molecules inside AFI crystal nano-channel, nevertheless iodine molecules inside AEL crystal nano-channel can only adopt two configurations: "lying" along the channel axis or "standing up" inside the channel. For clarity, only standing iodine molecules are depicted in (b) and (e). The two iodine molecules in (f) and (g) are the same ones just viewed from two orthogonal directions illustrated in (d).

of iodine molecule is l_d = 6.7 Å and the width is w_a = 4.0 Å, it can be inferred that iodine molecules may have any orientations inside the AFI crystal channel. They can "stand," "lie" or be placed in a certain angle with the channel axis anywhere inside the channel (Figure 2c). There is not a preferred orientation or favorite position for iodine molecules inside AFI crystal channels.

However, the situation is different for I_2@AEL. Unlike the AFI crystal, the cross section of the AEL crystal nano-channel is elliptical (Figure 2d, e). Figure 2f, g show the lateral views of Connolly surface observed from [010] and [100] directions with the observation directions illustrated in Figure 2d. Figure 2f illustrates that the major axis of the elliptical cross section fluctuates between d_l = 7.6 and d_s = 5.7 Å. It can be imagined that the iodine molecules may be oriented to "lie" along the channel axis or "stand" exactly at the widest part of the major axis (Figure 2f). The "lying" molecules can move back and forth inside the nano-channel, whilst the "standing" ones are trapped by the structure of the wide part. The minor axis fluctuates between d_l = 5.8 and d_s = 4.2 Å (Figure 2g). The iodine molecules cannot be oriented along the minor axis, so we can only see the vibrational motion of the "standing" and "lying" molecules in Figure 2e, g. It must be emphasized that the "lying" molecules are at the center of the channel, due to the shape of the elliptical cross section, actually they are hard to rotate even viewing from the same direction as that of Figure 2f (see also the Supporting Information). The transformation of iodine molecules from the "lying" to the "standing" ones are difficult, and vice versa. They must overcome the rotational energy barrier. In fact, the configurations of iodine molecules in Figure 2 are all based on the results of DFT calculations, which will be discussed in detail later. The van der Waals spheres representation in Figure 2 just well reproduces the electron density region within 0.033 electrons Å^{-3} (see the Supporting Information). The illustration of the size of the Connolly surface of the nano-channels just helps us to better understand the results of the DFT calculations.

2.2. The Normalized Raman Scattering Tensor

Polarized Raman spectroscopy was utilized to study the orientations of iodine molecules confined in the AFI and AEL single crystals. For experimental geometry in which the scattering and excitation lights are polarized along the ρ-axis and σ-axis, respectively, the Raman scattering intensity is proportional to the square of $\alpha'_{\rho\sigma}$, i.e., $I_{\rho\sigma} \propto \alpha'^2_{\rho\sigma}$ (the Supporting Information). Even though the number of molecules detected cannot be easily estimated, the relative value of the Raman scattering tensor α' can be determined straightforwardly.

From Equation (2), we can easily define a normalized $\overline{\alpha'_z}$ as

$$\overline{\alpha'_z} = \begin{bmatrix} 0.20 & 0 & 0 \\ 0 & 0.20 & 0 \\ 0 & 0 & 1.00 \end{bmatrix} \quad (5)$$

The correlated normalized scattering intensity tensor $\overline{I_z}$ is

$$\overline{I_z} = \begin{bmatrix} \overline{\alpha'^2_{xx}} & \overline{\alpha'^2_{xy}} & \overline{\alpha'^2_{xz}} \\ \overline{\alpha'^2_{yx}} & \overline{\alpha'^2_{yy}} & \overline{\alpha'^2_{yz}} \\ \overline{\alpha'^2_{zx}} & \overline{\alpha'^2_{zy}} & \overline{\alpha'^2_{zz}} \end{bmatrix} = \begin{bmatrix} 0.04 & 0 & 0 \\ 0 & 0.04 & 0 \\ 0 & 0 & 1.00 \end{bmatrix} \quad (6)$$

Equation (6) shows that, for the VV configuration (the polarizations of laser and Raman scattering lights are parallel) of an iodine molecule oriented along the z-axis, only $\overline{I_{zz}}$ dominates while $\overline{I_{xx}}$ and $\overline{I_{yy}}$ are much smaller. For the VH configuration (the polarizations of laser and Raman scattering lights are perpendicular), the Raman intensity should equal zero. So we would firstly use the VV configuration to determine whether the iodine molecules are oriented to a certain direction, if the answer is yes, the VH configuration will be adopted to further corroborate the Raman tensor of the orientation-fixed molecules. Compared with the free iodine molecules, the variation of Raman scattering tensor of the confined iodine molecules is very small and almost undetectable (see the Supporting Information). The change of Raman tensor is not considered here.

2.3. The Raman Spectra of "Disordered Gas"

Figure 3a shows the configuration of polarized Raman experiment on the flat-lying I_2@AFI. The crystal is put onto a rotation stage. Figure 3b shows the baseline corrected Raman spectra measured with different polarization angle α every 15° within 90°. It shows that only one Raman mode centered at 209.6 cm^{-1} is discernible. This is consistent with our assumption: iodine molecules can have any orientations inside the AFI crystal channel (Figure 2c). There is not a preferred orientation for iodine molecules. Figure 3c shows the polar graph of the corresponding normalized Raman intensities for a complete rotation. It reveals that the random distribution of iodine molecules is affected to some extent due to the existence of the nano-channel (the Supporting Information).

Figure 3d shows the Raman configuration on the erect I_2@AFI. Figure 3e illustrates that only one Raman mode centered at 209.6 cm^{-1} is observed. The normalized intensities shown in Figure 3f indicates that iodine molecules seem to be oriented randomly viewing from this direction, and the circular cross section shown in Figure 2b can further support this deduction.

In general, for I_2@AFI, the behavior of iodine molecules is similar to that of free-rotating gaseous molecules. The Raman tensor cannot be obtained from I_2@AFI. In contrast, the exact form of Raman tensor can be measured on I_2@AEL, in which the iodine molecules' orientations are determinate.

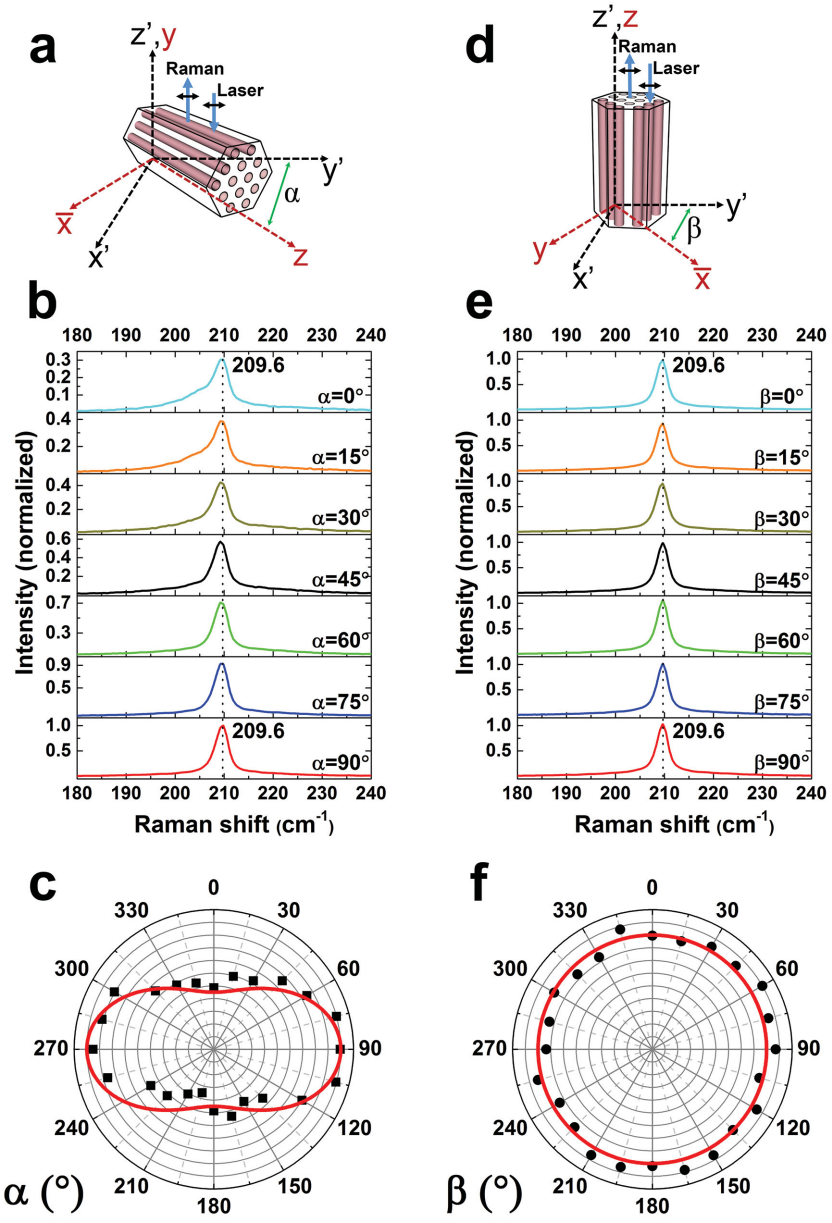

Figure 3. Polarized Raman experiments on the iodine-loaded AFI crystals. The configurations of the Raman experiments on a) flat-lying and d) erect AFI crystals are demonstrated. The incident excitation laser propagates along the $\overline{z'}$-axis and is polarized along the y'-axis. The backscattering Raman signal propagates along the z'-axis and is also polarized along the y'-axis (VV configuration). In addition to the laboratory coordinate system $x'y'z'$, the crystal coordinate system xyz is also indicated in red color. The polarization angles are denoted by α and β. The Raman spectra measured under each configuration with polarization angle within 90° are illustrated in (b) and (e), respectively. The corresponding normalized integrated intensities for one complete rotation are plotted with polar angles in (c) and (f), respectively, and the fitting curves are plotted in red color. It shows that only a Raman mode centered at 209.6 cm^{-1} is observed and the polarized characteristic is unobvious, so the behavior of the iodine molecules embedded in AFI crystal nano-channels is similar to that of "disordered gas."

2.4. The Raman Spectra of "Oriented Gas"

Figure 4a shows the Raman configuration on the flat-lying I_2@AEL. In this configuration the "view" of the channel

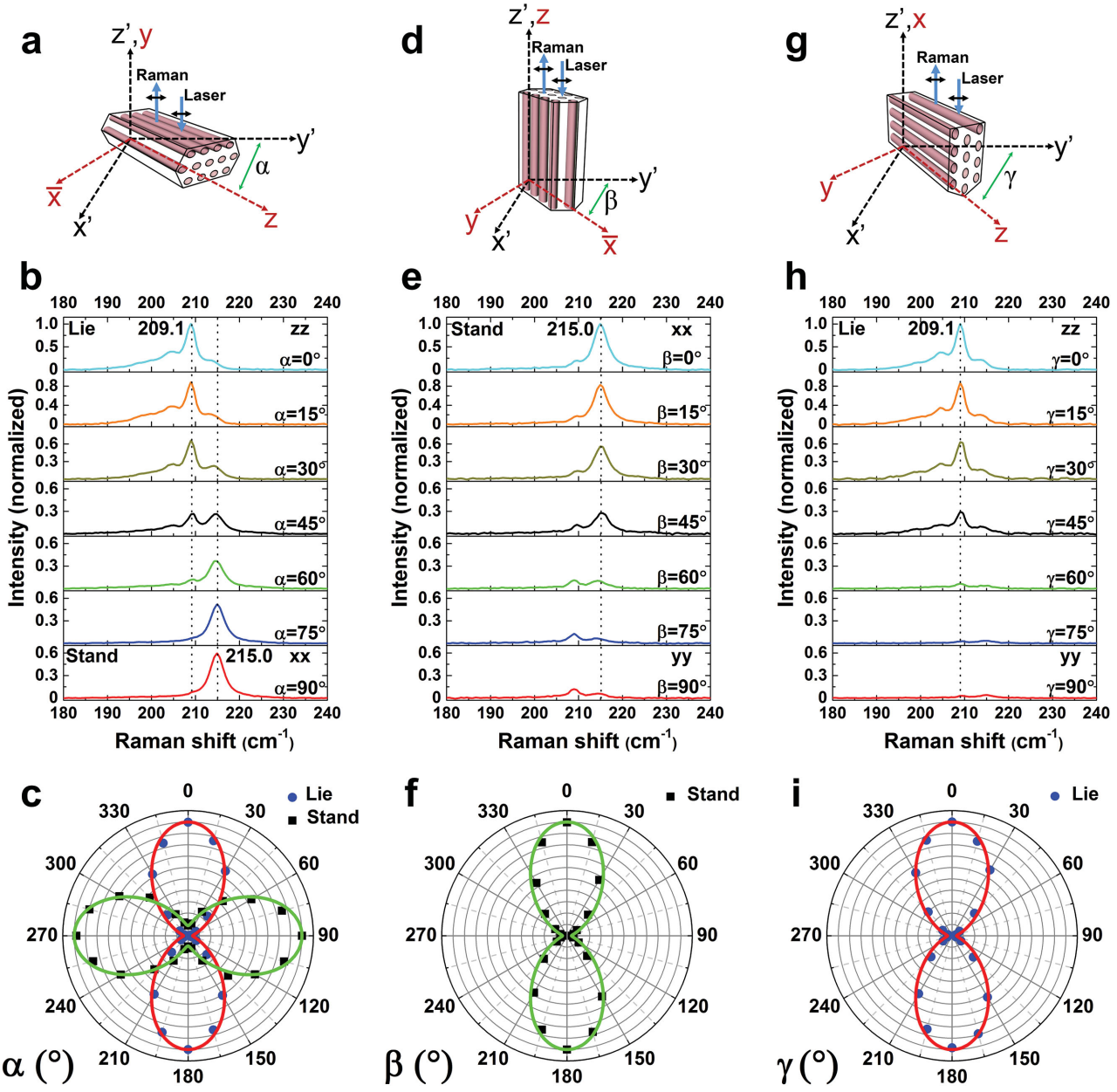

Figure 4. Polarized Raman experiments on the iodine-loaded AEL crystals. The configurations of the Raman experiments on a) flat-lying, d) erect, and g) side-lying AEL crystals are demonstrated. The incident excitation laser propagates along the $\overline{z'}$-axis and is polarized along the *y*′-axis. The backscattering Raman signal propagates along the *z*′-axis and is also polarized along the *y*′-axis (VV configuration). In addition to the laboratory coordinate system *x*′*y*′*z*′, the crystal coordinate system xyz is also indicated in red color. The polarization angles are denoted by α, β, and γ. The Raman spectra measured under each configuration with polarization angle within 90° are illustrated in b), e), and h), respectively. The corresponding normalized integrated intensities for one complete rotation are plotted with polar angles in c), f), and i), respectively. It shows that two Raman modes centered at 209.1 and 215.0 cm^{-1} are observed, which can be attributed to the "lying" and "standing" iodine molecules, respectively. The polarized characteristic is very obvious, so the "oriented gas" is formed inside the nano-channels of AEL crystals.

"seeing" from the laser is the same as Figure 2f. Figure 4b shows that two distinct Raman modes centered at 209.1 and 215.0 cm^{-1} are discernible with changing the polarization angle α from 0° to 90°. At α = 0°, only a Raman mode centered at 209.1 cm^{-1} is observed, which must correspond to the "lying" iodine molecules. Similarly, when α = 90°, the observed Raman mode centered at 215.0 cm^{-1} is ascribed to the "standing" molecules. With the increase of α from 0° to 90°, the Raman mode 209.1 cm^{-1} is gradually decreased and the mode 215.0 cm^{-1} is gradually increased. So there are indeed only two configurations of iodine molecules inside the AEL crystal channel: "standing" up or "lying" along the channel. The iodine molecules lose the "gas" characteristic and "oriented gas" is formed.

Table 1. Comparison between the characteristics of free and confined iodine molecules.

Configuration	Observed Raman shift [cm^{-1}]	Calculated Raman shift [cm^{-1}]	Calculated bond length [Å]	Calculated total energy of the system [eV]
Standing (AEL)	215.0	223.4	2.678	–77 083.6504
Lying (AEL)	209.1	219.9	2.684	–77 083.7639
Standing (AFI)	209.6	220.5	2.685	–46 495.5213
45°-tilted (AFI)	209.6	220.5	2.685	–46 495.5408
Lying (AFI)	209.6	220.4	2.685	–46 495.5414
Free state	213.3	220.7	2.685	

Figure 4c shows the corresponding normalized Raman intensities for a complete rotation. The rotation plane is the *xz*-plane, and the "lying" molecules are along the *z*-axis, while the "standing" ones are along the *x*-axis. Referring to Equation (3), if the molecule's orientation is fixed, its Raman intensity dependence on the rotation angle α can be expressed by the equation in form of $\overline{I(\alpha)} = \left[\alpha'_{\perp}\sin^2(\alpha+\delta) + \alpha'_{\parallel}\cos^2(\alpha+\delta)\right]^2$. Obviously the intensities of "lying" molecules can be fitted by the expression: $\overline{I(\alpha)} = \left(0.2\times\sin^2\alpha + \cos^2\alpha\right)^2$, which is represented by the red curve in Figure 4c. This is consistent with $\alpha'_{\perp} = 0.20, \alpha'_{\parallel} = 1.00$ of the normalized Raman tensor $\overline{\alpha'_z}$ expressed in Equation (5). The intensities of "standing" molecules can be fitted by $\overline{I(\alpha)} = \left[0.3\times\sin^2(\alpha+90°) + \cos^2(\alpha+90°)\right]^2$, which is represented by the green curve. The $\alpha'_{\perp} = 0.3$ is a little larger, which may be due to a slightly broad distribution of "standing" molecules instead of "standing" exactly along the major axis. This will be discussed in detail later.

Figure 4d shows the Raman configuration on the erect I_2@AEL. In this configuration the "view" of the channel "seeing" from the laser is the cross section as shown in Figure 2e. The "standing" molecules prevail, in comparison with that the signal for the "lying" ones is weak (Figure 4e). With the increase of the polarization angle β from 0° to 90°, the height of the "standing" Raman mode 215.0 cm^{-1} is gradually decreased. The intensities shown in Figure 4f can be well fitted by the expression $\overline{I(\beta)} = \left(0.2\times\sin^2\beta + \cos^2\beta\right)^2$, which is represented by the green curve.

Figure 4g shows the Raman configuration on the flank-ground I_2@AEL. The AEL crystal is stuck on a ceramic sheet to "stand" up and ground by a grinding/polishing machine. One flank of the AEL crystal as well as the ceramic sheet would be ground together to become a flat surface. The "lateral view of the laser" is illustrated in Figure 2g. Only the signal of the "lying" molecules is significant (Figure 4h). The intensities shown in Figure 4i can be well fitted by the expression $\overline{I(\gamma)} = \left(0.2\times\sin^2\gamma + \cos^2\gamma\right)^2$, which is plotted as the red curve.

2.5. The Density Functional Theory Calculation

Until now, all the Raman spectra have been interpreted perfectly, but it is just based on the analysis between the nano-channel's dimensions and the size of iodine molecules. In order to further understand the behavior of iodine molecules, DFT calculation is adopted to investigate the iodine molecules' stable configurations inside the nano-channels.

As mentioned before, the configurations of iodine molecules in Figure 2 are all depicted based on the results of DFT calculations. With the randomly initial placement of iodine molecule into the nano-channel of AEL crystal, tens of geometry optimization had been performed and only two stable configurations with local energy minima were found (Figure 2f, g). Not surprisingly, these two configurations correspond to the "standing" and "lying" iodine molecules. For I_2@AFI, the geometry optimization turns out that infinitely stable configurations with local energy minima exist. The AFI crystal's nano-channel only applies very weak influence on the iodine molecules embedded. Iodine molecules can almost be placed in any angle with the channel axis anywhere inside the channel.

The vibrational frequencies, bond lengths and total energies of free-standing molecules, "standing" and "lying" molecules for I_2@AEL and I_2@AFI as well as a 45°-tilted molecule for I_2@AFI are calculated, which are tabulated into **Table 1**. Because iodine molecules can have any orientation inside the nano-channel of AFI crystal, only "standing," "lying," and "45°-tilted" ones are sampled. For confined molecules, experimental results indicate that the observed Raman modes except the "standing" one for I_2@AEL are all around 210 cm^{-1}, which can be regarded as a natural vibrational frequency of iodine molecules inside the nano-channels. The DFT calculations show the same result that the natural vibrational mode is around 220 cm^{-1}. For the "standing" molecules of I_2@AEL, there is a blueshift of about 5 cm^{-1} for the observed Raman mode, and for the calculation results, the blueshift is around 3 cm^{-1}. Generally speaking, apart from the systematic error, the calculated and observed Raman shifts are consistent with each other. In view of the DFT calculation results, the prior explanations of the polarized Raman spectra are completely correct.

Table 1 also indicates that calculated natural bond length of the confined molecules is about 2.685 Å, which is just a little larger than the experimental value 2.665 Å of free-standing iodine molecule.[32] In comparison with the natural length 2.685 Å, the bond length 2.678 Å of the "standing" molecule for I_2@AEL is a little shorter, which is due to the compression effect of the channel framework on the "standing" molecule (Figure 2f). This compression effect also leads to the blueshift of the observed Raman mode from 209.1 cm^{-1} of "lying" molecule to 215.0 cm^{-1} or the calculated Raman mode from 219.9 to 223.4 cm^{-1}.

2.6. The Raman Scattering Tensor Determination

The experimental results are well understood now. For I_2@AEL, the iodine molecules would indeed either "lie" or "stand"

inside the nano-channel, so the Raman scattering tensor can be measured directly. The diagonal terms of normalized scattering intensity tensors of the "lying" and "standing" iodine molecules for I_2@AEL have been determined as

$$\overline{I_{\text{lie}}} = \begin{bmatrix} 0.04 & * & * \\ * & 0.04 & * \\ * & * & 1.00 \end{bmatrix}, \overline{I_{\text{stand}}} = \begin{pmatrix} 1.00 & * & * \\ * & 0.04 & * \\ * & * & 0.09 \end{pmatrix} \quad (7)$$

The remaining task is to determine the off-diagonal terms. **Figure 5**b shows six normalized spectra in the crossed scattering polarization geometries (VH configuration) for I_2@AEL. The normalized spectrum of *yy* polarization geometry which relates to $\overline{\alpha'^2_{\perp}}$ in VV configuration is also plotted for comparison. In general, for "lying" iodine molecules, all the off-diagonal terms are less than or comparable to 0.01. This implies that the lying molecules will have a standard deviation of 5° to 10° at room temperature (the Supporting Information). If we neglect this small deviation and regard all the off-diagonal terms of lying molecules as zero, the normalized Raman scattering tensor $\overline{\alpha'_{\text{lie}}}$ of "lying" iodine molecules can be expressed as

$$\overline{\alpha'_{\text{lie}}} = \begin{bmatrix} 0.2 & 0 & 0 \\ 0 & 0.2 & 0 \\ 0 & 0 & 1.0 \end{bmatrix} \quad (8)$$

which is exactly the same as the one obtained from DFT calculation as shown in Equation (5). It demonstrates that the Raman tensor, for the first time, can be verified directly on the orientation-fixed molecules at room temperature.

While for "standing" iodine molecules, it is obvious that the *xz* and *zx* terms of intensity tensor are nonzero (Figure 5b). The normalized scattering intensity tensor can be expressed as

$$\overline{I_{\text{stand}}} = \begin{bmatrix} 1.00 & 0 & 0.05 \\ 0 & 0.04 & 0 \\ 0.05 & 0 & 0.09 \end{bmatrix} \quad (9)$$

This contradiction to group theory is due to the distribution influence and can be understood as follows: The "standing" molecules would like to try to get rid of the compression exerted by the channel framework, so their orientations are not exactly along the major axis shown in Figure 2f. Here we model that the "standing" molecules inside the trap will have a normal distribution centered at the standing direction with a standard deviation of $\sigma = 18°$ (the Supporting Information). The normalized scattering intensity tensor can be calculated as

$$\overline{I_{\text{stand}}} = \int_{-\pi}^{\pi} \frac{1}{\sigma\sqrt{2\pi}} \exp\left(-\frac{\theta^2}{2\sigma^2}\right) \begin{bmatrix} \left(\overline{\alpha'_{\perp}}\sin^2\theta + \overline{\alpha'_{\parallel}}\cos^2\theta\right)^2 & 0 & \left(\overline{\alpha'_{\perp}} - \overline{\alpha'_{\parallel}}\right)^2 \sin^2\theta\cos^2\theta \cdot \\ 0 & \overline{\alpha'^2_{\perp}} & 0 \\ \left(\overline{\alpha'_{\perp}} - \overline{\alpha'_{\parallel}}\right)^2 \sin^2\theta\cos^2\theta & 0 & \left(\overline{\alpha'_{\perp}}\cos^2\theta + \overline{\alpha'_{\parallel}}\sin^2\theta\right)^2 \end{bmatrix} = \begin{bmatrix} 1.00 & 0 & 0.05 \\ 0 & 0.04 & 0 \\ 0.05 & 0 & 0.09 \end{bmatrix} \quad (10)$$

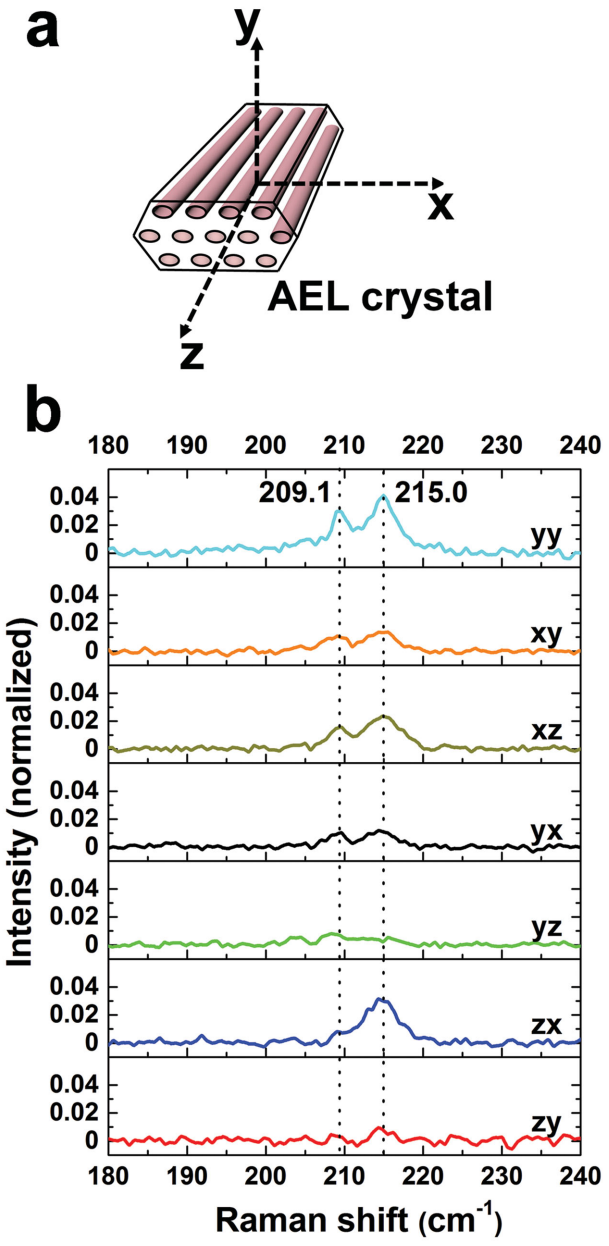

Figure 5. The determination of the off-diagonal terms of Raman scattering tensors of the confined "lying" and "standing" iodine molecules in the iodine-loaded AEL crystal. The coordinate system *xyz* on the AEL crystal is defined in a). The six normalized Raman spectra in VH configurations to evaluate the off-diagonal terms are plotted in b). The normalized spectrum for the *yy* polarization geometry which is measured in VV configuration is also plotted for comparison. It shows that for "lying" iodine molecules, all the off-diagonal terms can be regarded as zero. In contrast, for "standing" iodine molecules, the *xz* and *zx* terms are nonzero.

which is exactly the same as that shown in Equation (9). The actual distribution function may be complicated, this assumption just gives a simple instance that Raman tensor can also be used to estimate the molecules' orientation distribution. For "lying" molecules, the experimental results have suggested that they can be regarded as lying exactly along the

channel axis, the observed Raman tensor is in good agreement with theoretical value obtained from DFT calculation. This work is the first clear demonstration that Raman scattering tensor of single molecules can be measured directly and completely.

3. Conclusions

In summary, we have proposed and demonstrated an approach to directly measure the Raman scattering tensor of single molecules. From the comparison between the polarized Raman spectroscopy and DFT calculation on iodine molecules inside AEL and AFI crystals' nano-channels, it is revealed that the iodine molecules inside AFI crystal behave similarly to "disordered gas", while the iodine molecules inside AEL crystal resemble the "oriented gas." The orientation-fixed molecules in AEL crystal offer us such an unprecedented opportunity to directly measure their Raman scattering tensor, and the experimental value obtained is in excellent agreement with the one predicted from DFT calculations. We want to emphasize that iodine molecules just serve as a very simple demonstration. Taking the whole 225 known zeolite framework types into account, a great deal of target molecules can be analyzed. Even for AFI and AEL crystals alone, dozens of candidates still exist. In addition to zeolite crystals, other matrix crystals or novel 3D nano-devices may also serve as promising alternatives.[38] Our work demonstrated that by carefully choosing the relevant zeolite crystals with appropriate nano-space, the big family of zeolites can be utilized as directing template database for orientating a large number of guest molecules to determine their Raman scattering tensors, which can be used to estimate the molecular structure containing the target guest molecules as functional groups.

4. Experimental Section

Preparation of I_2@AEL and I_2@AFI Crystals: The AFI and AEL single crystals were crystallized by using hydrothermally template-directed synthesis method.[39,40] The typical dimensions of the as-synthesized AFI and AEL single crystals are $100 \times 100 \times 300$ and $10 \times 30 \times 80$ μm, respectively. The organic template molecules occluded in the nano-channels were removed by calcining the crystals in oxygen atmosphere for about 20 h. The iodine molecules could be diffused into the nano-channels by sealing the calcined crystals and solid iodine source (BDH laboratory supplies, >99%) together in a Pyrex tube under a vacuum of 10^{-3} mbar. The loading density of iodine molecules in the nano-channels can be controlled by the weight ratio of the loaded solid iodine to the AFI or AEL single crystals. We only concentrate on the low-density iodine-loaded AEL and AFI crystals in this work.

Raman Scattering Experiment: Polarized Raman spectra were measured at room temperature using Jobin-Yvon T64000 micro-Raman spectrometer in a backscattering configuration, which is equipped with a CCD detector cooled by liquid nitrogen. The excitation laser line is a linearly polarized 514.5 nm beam generated from an Innova 70C Spectrum laser with a line width of 6 GHz and a power of 30 mW. A l00× microscope objective was employed to focus the laser spot onto the samples. Subpixel acquisition function of T64000 spectrometer was adopted to determine the peak position with a precision up to 0.1 cm^{-1}. For I_2@AEL, the Raman spectra were resolved into the "standing" and "lying" modes based on the Lorentzian line shape analysis. The intensities were calculated based on the integrated areas.

The Connolly Surface of the Nano-Channels: Connolly surface shown in Figure 2, which is the "accessible surface" of iodine atom, was calculated via a rolling ball algorithm.[37] It depends on the atomic coordinates and van der Waals radii of the framework atoms as well as the atomic radius of the probe atom. Since there is a 10% uncertainty of the van der Waals radii of the atoms,[32] Connolly surface only roughly illustrates the characteristic of the nano-channel. The radii of framework atoms are taken from Mantina's values:[41] 1.84, 1.80, and 1.52 Å for aluminum, phosphorus, and oxygen, respectively. The radius of the probe atom is set to equal the iodine's atomic radius: 1.98 Å.

The DFT Calculation: The first-principles DFT calculation was performed by using the CASTEP plane-wave code which has been integrated into Materials Studio 6.0 suite package. The exchange-correlation potential was treated within the generalized gradient-corrected approximation (GGA) by the Wu--Cohen (WC) functional.[42] Norm-conserving pseudopotentials[43] (NCP) of the phosphorus, aluminum, oxygen, and iodine atoms were generated by using the open source pseudopotential generation package Opium 3.7. The calculation details are provided in the Supporting Information.

Supporting Information

Supporting Information is available from the Wiley Online Library or from the author.

Acknowledgements

D.W. wants to thank Haijing Zhang of Hong Kong University of Science and Technology for many meaningful discussions. The authors thank the National Supercomputing Center in Shenzhen (China) for providing the Materials Studio 6.0 suite package and the supercomputing service. This work was supported by Hong Kong CERGC Grant 604210.

Received: February 25, 2015
Revised: April 13, 2015
Published online: May 21, 2015

[1] D. A. Long, *The Raman Effect: A Unified Treatment of the Theory of Raman Scattering by Molecules*, John Wiley & Sons, Ltd., **2002**, p. 85.
[2] J. M. Hollas, *Modern Spectroscopy*, John Wiley & Sons, Ltd., **2004**, p. 407.
[3] T. C. Damen, S. P. S. Porto, B. Tell, *Phys. Rev.* **1966**, *142*, 570.
[4] C. A. Arguello, D. L. Rousseau, S. P. S. Porto, *Phys. Rev.* **1969**, *181*, 1351.
[5] S. P. S. Porto, P. A. Fleury, T. C. Damen, *Phys. Rev.* **1967**, *154*, 522.
[6] G. S. Duesberg, I. Loa, M. Burghard, K. Syassen, S. Roth, *Phys. Rev. Lett.* **2000**, *85*, 5436.
[7] A. M. Rao, A. Jorio, M. A. Pimenta, M. S. S. Dantas, R. Saito, G. Dresselhaus, M. S. Dresselhaus, *Phys. Rev. Lett.* **2000**, *84*, 1820.
[8] R. Saito, T. Takeya, T. Kimura, G. Dresselhaus, M. S. Dresselhaus, *Phys. Rev. B* **1998**, *57*, 4145.
[9] A. Jorio, G. Dresselhaus, M. S. Dresselhaus, M. Souza, M. S. S. Dantas, M. A. Pimenta, A. M. Rao, R. Saito, C. Liu, H. M. Cheng, *Phys. Rev. Lett.* **2000**, *85*, 2617.
[10] M. Tsuboi, J. M. Benevides, G. J. Thomas, *Proc. Jpn. Acad., Ser. B* **2009**, *85*, 83.
[11] R. Intartaglia, K. Bagga, F. Brandi, G. Das, A. Genovese, E. Di Fabrizio, A. Diaspro, *J. Phys. Chem. C* **2011**, *115*, 5102.
[12] L. Gross, F. Mohn, N. Moll, P. Liljeroth, G. Meyer, *Science* **2009**, *325*, 1110.
[13] S. Nie, S. R. Emory, *Science* **1997**, *275*, 1102.

[14] K. Kneipp, Y. Wang, H. Kneipp, L. T. Perelman, I. Itzkan, R. R. Dasari, M. S. Feld, *Phys. Rev. Lett.* **1997**, *78*, 1667.
[15] R. Zhang, Y. Zhang, Z. C. Dong, S. Jiang, C. Zhang, L. G. Chen, L. Zhang, Y. Liao, J. Aizpurua, Y. Luo, J. L. Yang, J. G. Hou, *Nature* **2013**, *498*, 82.
[16] D. Porezag, M. R. Pederson, *Phys. Rev. B* **1996**, *54*, 7830.
[17] F. G. Alabarse, J. Haines, O. Cambon, C. Levelut, D. Bourgogne, A. Haidoux, D. Granier, B. Coasne, *Phys. Rev. Lett.* **2012**, *109*, 035701.
[18] N. Wang, Z. K. Tang, G. D. Li, J. S. Chen, *Nature* **2000**, *408*, 50.
[19] P. Demontis, J. Gulín-González, H. Jobic, M. Masia, R. Sale, G. B. Suffritti, *ACS Nano* **2008**, *2*, 1603.
[20] D. Verboekend, J. C. Groen, J. Pérez-Ramírez, *Adv. Funct. Mater.* **2010**, *20*, 1441.
[21] L. I. Devriese, L. Cools, A. Aerts, J. A. Martens, G. V. Baron, J. F. M. Denayer, *Adv. Funct. Mater.* **2007**, *17*, 3911.
[22] Z. K. Tang, J. P. Zhai, Y. Y. Tong, X. J. Hu, R. Saito, Y. J. Feng, P. Sheng, *Phys. Rev. Lett.* **2008**, *101*, 047402.
[23] F. Y. Jiang, R. C. Liu, *J. Phys. Chem. Solids* **2007**, *68*, 1552.
[24] J. P. Zhai, H. F. Lee, I. L. Li, S. C. Ruan, Z. K. Tang, *Nanotechnology* **2008**, *19*, 175604.
[25] J. P. Zhai, I. L. Li, S. C. Ruan, H. F. Lee, Z. K. Tang, *Appl. Phys. Lett.* **2008**, *92*, 043117.
[26] C. Minkowski, R. Pansu, M. Takano, G. Calzaferri, *Adv. Funct. Mater.* **2006**, *16*, 273.
[27] O. Nicolet, S. Huber, C. Lovey, S. Chappellet, J. Perrenoud, M. Pauchard, R. Ferrini, L. Zuppiroli, *Adv. Funct. Mater.* **2009**, *19*, 1877.
[28] Z. Li, G. Luppi, A. Geiger, H.-P. Josel, L. De Cola, *Small* **2011**, *7*, 3193.
[29] Z. M. Li, Z. K. Tang, H. J. Liu, N. Wang, C. T. Chan, R. Saito, S. Okada, G. D. Li, J. S. Chen, N. Nagasawa, S. Tsuda, *Phys. Rev. Lett.* **2001**, *87*, 127401.
[30] J. Guo, C. Yang, Z. M. Li, M. Bai, H. J. Liu, G. D. Li, E. G. Wang, C. T. Chan, Z. K. Tang, W. K. Ge, X. Xiao, *Phys. Rev. Lett.* **2004**, *93*, 017402.
[31] W. Guo, D. Wang, J. Hu, Z. K. Tang, S. Du, *Appl. Phys. Lett.* **2011**, *98*, 043105.
[32] D. Wang, W. Guo, J. Hu, F. Liu, L. Chen, S. Du, Z. Tang, *Sci. Rep.* **2013**, 3, 1486.
[33] D. Wang, W. Guo, S. Du, Z. K. Tang, *Mod. Phys. Lett. B* **2013**, *27*, 1330014.
[34] J. M. Bennett, J. P. Cohen, E. M. Flanigen, J. J. Pluth, J. V. Smith, *Intrazeolite Chemistry*, Vol. *218*, American Chemical Society, **1983**, p. 109.
[35] J. J. Pluth, J. V. Smith, J. W. Richardson, *J. Phys. Chem.* **1988**, *92*, 2734.
[36] J. W. Richardson, J. J. Pluth, J. V. Smith, *Acta Crystallogr. Sect. B* **1988**, *44*, 367.
[37] M. L. Connolly, *J. Appl. Crystallogr.* **1983**, *16*, 548.
[38] F. De Angelis, C. Liberale, M. L. Coluccio, G. Cojoc, E. Di Fabrizio, *Nanoscale* **2011**, *3*, 2689.
[39] F. Y. Jiang, J. P. Zhai, J. T. Ye, J. R. Han, Z. K. Tang, *J. Cryst. Growth* **2005**, *283*, 108.
[40] L. Fu, J. P. Zhai, J. M. Hu, I. L. Li, S. C. Ruan, Z. K. Tang, *Microporous Mesoporous Mater.* **2011**, *137*, 1.
[41] M. Mantina, A. C. Chamberlin, R. Valero, C. J. Cramer, D. G. Truhlar, *J. Phys. Chem. A* **2009**, *113*, 5806.
[42] Z. Wu, R. E. Cohen, *Phys. Rev. B* **2006**, *73*, 235116.
[43] D. R. Hamann, M. Schlüter, C. Chiang, *Phys. Rev. Lett.* **1979**, *43*, 1494.